



Contents lists available at ScienceDirect

## Bioorganic &amp; Medicinal Chemistry Letters

journal homepage: [www.elsevier.com/locate/bmcl](http://www.elsevier.com/locate/bmcl)

## New amide linked dimeric 1,2,3-triazoles bearing aryloxy scaffolds as a potent antiproliferative agents and EGFR tyrosine kinase phosphorylation inhibitors

Tejshri R. Deshmukh<sup>a</sup>, Aniket P. Sarkate<sup>b</sup>, Deepak K. Lokwani<sup>c</sup>, Shailee V. Tiwari<sup>d</sup>, Rajaram Azad<sup>e</sup>, Bapurao B. Shingate<sup>a,\*</sup>

<sup>a</sup> Department of Chemistry, Dr. Babasaheb Ambedkar, Marathwada University, Aurangabad 431 004, Maharashtra, India

<sup>b</sup> Department of Chemical Technology, Dr. Babasaheb Ambedkar Marathwada University, Aurangabad 431 004, Maharashtra, India

<sup>c</sup> Department of Pharmaceutical Chemistry, R.C. Patel Institute of Pharmaceutical Education & Research, Shirpur 425 405, Maharashtra, India

<sup>d</sup> Department of Pharmaceutical Chemistry, Durgamata Institute of Pharmacy, Dharmapuri, Parbhani 431 401, Maharashtra, India

<sup>e</sup> Department of Animal Biology, University of Hyderabad, Hyderabad 500 046, India

## ARTICLE INFO

## Keywords:

Antiproliferative activity

Click reaction

Dimeric 1,2,3-triazoles

EGFR tyrosine kinase phosphorylation inhibition

Molecular docking study

## ABSTRACT

A search for potent antiproliferative agents has prompted to design and synthesize aryloxy bridged and amide linked dimeric 1,2,3-triazoles (**7a–j**) by using 1,3-dipolar cycloaddition reaction between 2-azido-*N*-phenylacetamides (**4a–e**) and bis(prop-2-yn-1-yloxy)benzenes (**6a–b**) via copper (I)-catalyzed click chemistry approach with good to excellent yields. All the newly synthesized compounds have been screened for their *in vitro* antiproliferative activities against two human cancer cell lines. The compounds **7d**, **7e**, **7h**, **7i** and **7j** have revealed promising antiproliferative activity against human breast cancer cell line (MCF-7), whereas, the compounds **7a**, **7b**, **7c**, **7i** and **7j** were observed as potent antiproliferative agents against human lung cancer cell line (A-549). The active compounds against MCF-7 have been also analysed for their mechanism of action by the enzymatic study, which shows that the compounds **7d**, **7h** and **7j** were acts as active EGFR tyrosine kinase phosphorylation inhibitors. In support to this biological study, the molecular docking as well as *in silico* ADME properties of all the newly synthesized hybrids were predicted.

Cancer is a life threatening disease that originates when there is an imbalance in cellular signals, which generally controls the cell proliferation, growth, morphogenesis and apoptosis.<sup>1</sup> These signals were mainly regulated by the enzymes, ‘Tyrosine Kinases’ by the phosphorylation of tyrosine residue in different substrates.<sup>2</sup> There are certain receptors available for these kind of substrates, which plays a key role in the genesis of many kind of cancers. ‘Epidermal Growth Factor Receptor’ (EGFR) is one of them, which activates tyrosine kinase phosphorylation after the binding of ligands by dimerization.<sup>3</sup> Thus, to control the growth of cancerous cells by balancing cellular signals, it is necessary to inhibit those activated dimeric species of EGFR. Literature survey reveals that, the dimeric drug can shows better binding affinity to inhibit the activated dimeric species of EGFR rather than two separate monomeric drugs.<sup>4</sup> Therefore, we have synthesized the series of dimeric compounds with hope to obtain better EGFR tyrosine kinase phosphorylation inhibitors as well as antiproliferative agents.

Recently, many antiproliferative agents were reported with the

azole motif in their molecular framework.<sup>5a–c</sup> Mostly, the development of new antiproliferative agents bearing 1,4-disubstituted 1,2,3-triazole as a pharmacophoric unit is being highlighted by many researchers.<sup>6a–d</sup> The 1,4-disubstituted 1,2,3-triazoles are easy to synthesize by using Cu (I)-catalyzed 1,3-dipolar cycloaddition reaction in between azide and alkyne with the help of Sharpless and Meldal’s greener approach of click chemistry.<sup>7</sup> They are acts as bioisostere of amide bond, therefore, it shows high binding affinity to many biological targets.<sup>8</sup> Similarly, etheral as well as amide functionalities are also tends to interact with various biological targets. Here, we have shown some molecular structures of antiproliferative agents bearing amide and etheral linked 1,2,3-triazolyl scaffolds<sup>9–12</sup> in Fig. 1.

Considering the therapeutic significance of the above, herein, we have planned and synthesized dimeric 1,2,3-triazoles by accumulating amide linked substituted variant unit, dimeric 1,2,3-triazoles and aryloxy moiety in a single molecular framework with hope to obtain better antiproliferative agents with reduced side effects.

\* Corresponding author.

E-mail address: [bapushingate@gmail.com](mailto:bapushingate@gmail.com) (B.B. Shingate).

<https://doi.org/10.1016/j.bmcl.2019.08.022>

Received 26 May 2019; Received in revised form 10 August 2019; Accepted 11 August 2019

0960-894X/ © 2019 Elsevier Ltd. All rights reserved.

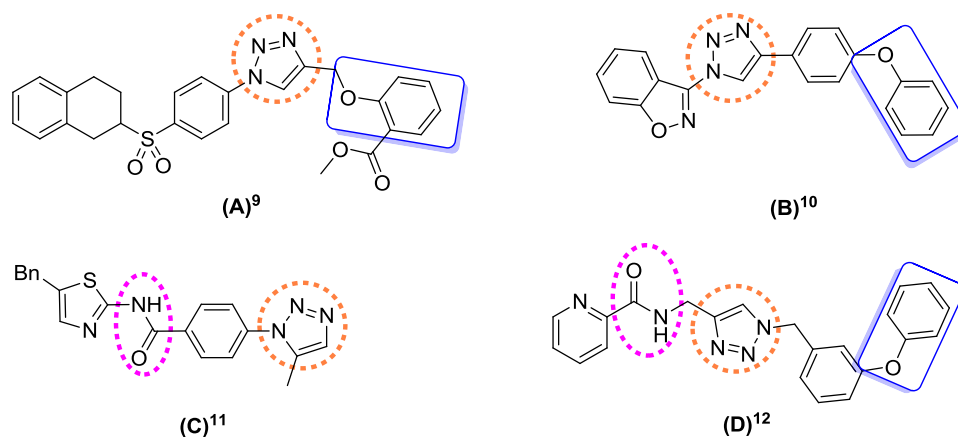


Fig. 1. Ether and amide linked 1,2,3-triazolyl scaffolds as antiproliferative agents.

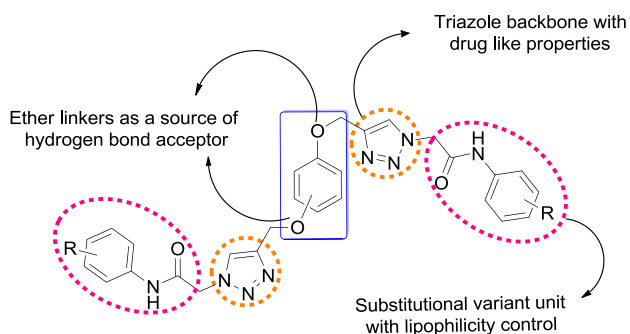


Fig. 2. Molecular design strategy for the synthesis of novel dimeric 1,2,3-triazole derivatives bearing aryloxy scaffolds.

The design of aryloxy bridged and amide linked substituted dimeric 1,2,3-triazoles hybrids was broadly divided into three segments as shown in Fig. 2. The first one is the main backbone of the design strategy, that is symmetrically situated two 1,2,3-triazolyl units. It helps to enhance the pharmacophoric properties as they exhibits drug like properties. The second segment is 1,2 or 1,3-diaryloxy moiety showing etheral linkages with triazolyl units as a source of hydrogen bond acceptor. Lastly, the substituted 1,2,3-triazolyl acetamide fragment with substitutional variant unit, which was generally used to control the lipophilicity as well as it contributes as the most active pharmacophoric unit due to presence of amide linkage.

The synthesis of new aryloxy bridged and amide linked substituted dimeric 1,2,3-triazoles (**7a–j**) were carried out *via* multi-step synthetic pathway as illustrated in Schemes 1–3. The desired compounds (**7a–j**) were synthesized by using copper(I)-catalyzed click reaction as described in Scheme 3. The required starting material, 2-azido-*N*-phenylacetamide derivatives (**4a–e**) were prepared from corresponding anilines (**1a–e**) *via* chloro acylation reaction followed by treatment with sodium azide as depicted in Scheme 1.<sup>13</sup>

The another precursors, 1,3-bis(prop-2-yn-1-yloxy)benzene (**6a**) and 1,2-bis(prop-2-yn-1-yloxy)benzene (**6b**) were synthesized from resorcinol (**5a**) and catechol (**5b**), respectively. The compounds (**5a**) and (**5b**) were separately allowed to react with propargyl bromide in presence of  $K_2CO_3$  as a base in *N,N*-dimethylformamide (DMF) at room temperature<sup>14</sup> resulted in good to excellent yields of dialkynes (**6a**) and (**6b**), respectively (Scheme 2).

The desired aryloxy bridged and amide linked dimeric 1,2,3-triazoles (**7a–j**) were synthesized by 1,3-dipolar cycloaddition reaction of freshly synthesized 2-azido-*N*-phenylacetamide derivatives (**4a–e**) with bis(prop-2-yn-1-yloxy)benzene (**6a–b**) as a source of dialkyne. This click reaction was carried out in presence of catalytic amount of  $CuSO_4 \cdot 5H_2O$  and sodium ascorbate in PEG-400:H<sub>2</sub>O (3:1) for 8 h at

room temperature resulted into the corresponding aryloxy bridged and amide linked dimeric 1,2,3-triazoles (**7a–j**) in excellent yields (Scheme 3).

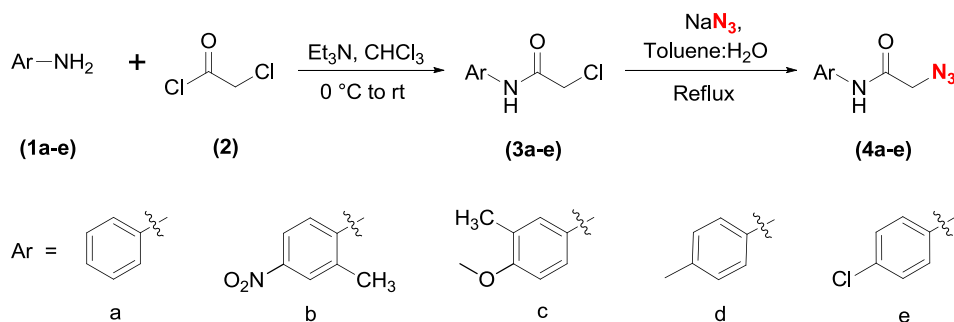
The structures of all the newly designed and synthesized dimeric 1,2,3-triazole derivatives (**7a–j**) bearing aryloxy scaffolds are shown in Fig. 3. All these compounds (**7a–j**) have been characterized by physical data and spectral analysis.<sup>15</sup>

All the newly synthesized aryloxy bridged and amide linked substituted dimeric 1,2,3-triazoles (**7a–j**) were evaluated for their *in vitro* antiproliferative activity against two human cancer cell lines as well as the inhibition of EGFR tyrosine kinase phosphorylation was also studied by comparing the results with standard antiproliferative drug, Gefitinib. *In vitro* antiproliferative screening of titled compounds against the human breast cancer cell line (MCF-7) and human lung cancer cell line (A-549) were performed using MTT assay.<sup>16</sup> The obtained results of *in vitro* antiproliferative activities are summarized in Table 1. The detailed study of *in vitro* antiproliferative with graphical representation have been shown in Supporting Information (Table S1 and Figs. S1, S2).

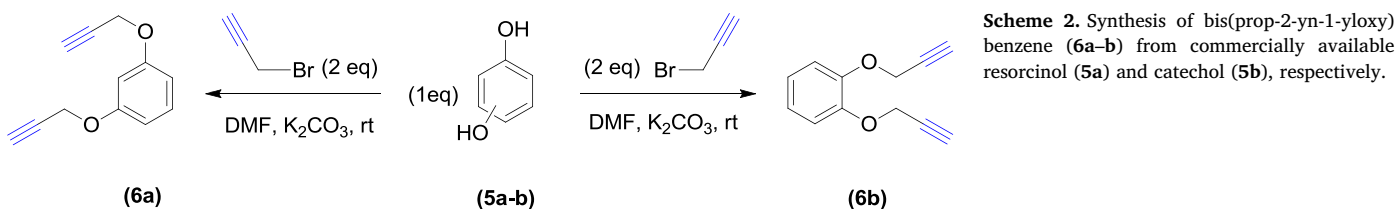
From Table 1, we can conclude that among all the newly synthesized compounds of the series, eight compounds have been displayed significant antiproliferative activities against tested human cancer cell lines MCF-7 and A-549. The compounds, **7d**, **7e**, **7h**, **7i** and **7j** have revealed promising antiproliferative activity against human breast cancer cell line (MCF-7), whereas, the compounds, **7a**, **7b**, **7c**, **7i** and **7j** were observed as potent antiproliferative agents against human lung cancer cell line (A-549). As most of compounds from series were shows potency against tested human cancer cell lines, we can conclude that the newly synthesized compounds offers an attractive lead series for the discovery of novel antiproliferative agents in future by generating more similar compounds and continuing further research on active compounds.

In this study, the compounds **7b** and **7c** were observed as the most potent antiproliferative agents from the series against A-549 as they exhibited antiproliferative activities with  $IC_{50}$  values 2.22  $\mu M$  and 2.34  $\mu M$ , respectively. The compounds **7i** and **7j** were having good antiproliferative activities against both the cancer cell lines, MCF-7 and A-549. The compound **7i** was displayed  $IC_{50}$  values 6.70 and 5.56  $\mu M$  whereas; the compound **7j** has shown  $IC_{50}$  values 2.80  $\mu M$  and 5.61  $\mu M$ , respectively against MCF-7 and A-549. Therefore, it was observed that the compound **7j** shows better antiproliferative activity against MCF-7 among the newly synthesized compounds of the series. In addition to this, some other compounds like **7d**, **7e** and **7h** were also display potency against MCF-7 with  $IC_{50}$  values 6.01  $\mu M$ , 6.13  $\mu M$  and 4.18  $\mu M$ , respectively. Furthermore, the compound **7a** was also found to be active against A-549 with  $IC_{50}$  value 7.05  $\mu M$ .

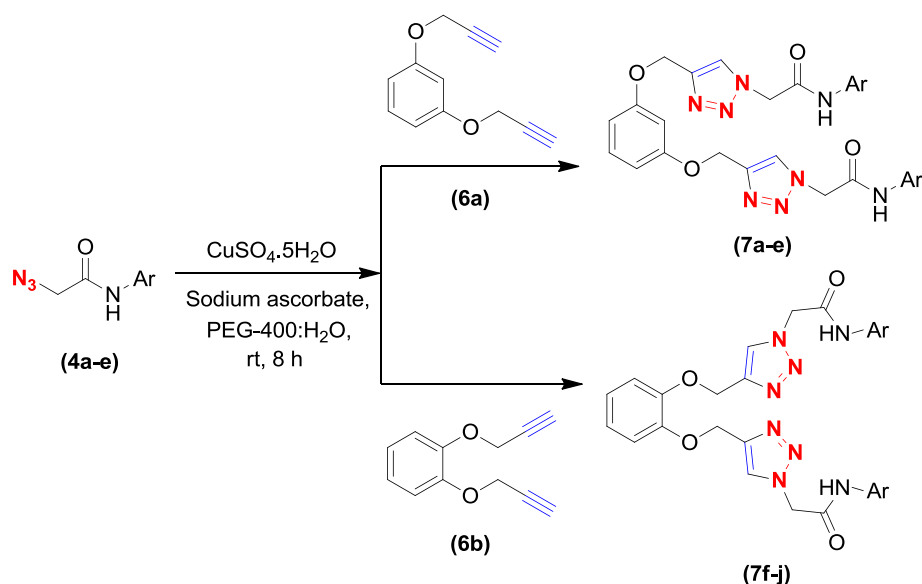
As we found that the compounds **7h** and **7j** were act as the most potent antiproliferative agents against MCF-7 cancer cell line, they are



**Scheme 1.** Synthesis of 2-azido-N-phenylacetamides (4a-e) via 2-chloro-N-phenylacetamides (3a-m) from respective aromatic amines (1a-e).



**Scheme 2.** Synthesis of bis(prop-2-yn-1-yloxy) benzene (6a-b) from commercially available resorcinol (5a) and catechol (5b), respectively.



**Scheme 3.** Synthesis of aryloxy and amide linked substituted dimeric 1,2,3-triazoles (7a-j).

also evaluated for study their cytotoxic nature against MCF-10A (normal breast epithelial cell line). This study helps to know the selectivity of these active compounds towards cancerous cells. If the compound is more selective towards cancerous cells then it must be less toxic to the normal cells. From the Table 1, it was observed that the compound 7h shows IC<sub>50</sub> value 33.44 μM against MCF-10A, which means that it shows eight times more selectivity towards MCF-7. Similarly, the compound 7j shows 5 times more selectivity towards MCF-7 cancer cell line as it displays IC<sub>50</sub> value 14 μM against MCF-10A. After this comparative study, we can conclude that the potent compounds from the newly synthesized series were more selective towards cancerous cells, whereas, they were very less toxic towards the normal breast epithelial cells.

From the above results, it was observed that most of the compounds from the series displays moderate to good antiproliferative activities. But the careful examination leads to the establishment of a significantly regular structure activity relationship (SAR), which indicates that, the presence of different substituents such as -NO<sub>2</sub>, -OCH<sub>3</sub>, -CH<sub>3</sub> and -Cl on the phenyl rings of compounds may responsible to enhance the

bioactivity, whereas, the compounds with no substituents observed as inactive. Specifically, the most potent compounds from series, 7j and 7b bearing -Cl and -NO<sub>2</sub> groups on the phenyl rings with catechol and resorcinol moieties, respectively as a source of aryloxy scaffolds may responsible for their highly potent biological activities.

In addition to this, to explicate the inhibition of cancer cells proliferation were associated with EGFR, the inhibition of EGFR tyrosine kinase phosphorylation was studied. 'Epidermal Growth Factor Receptor' (EGFR) is one of the receptor, that used to activates tyrosine kinase phosphorylation after the binding of ligands by dimerization.<sup>3</sup> Thus, to control the growth of cancerous cells, it is necessary to inhibit these activated dimeric species of EGFR. Literature survey reveals that, the dimeric drug can show better binding affinity to inhibit the activated dimeric species of EGFR rather than two separate monomeric drugs.<sup>4</sup> Therefore, we have evaluated only the potent antiproliferative agents of the newly synthesized series against MCF-7 using Western blot analysis.<sup>17</sup> Here, Gefitinib was used as a standard drug, as it was already a good inhibitor of EGFR tyrosine kinase phosphorylation. It shows the complete inhibition of the EGFR tyrosine kinase

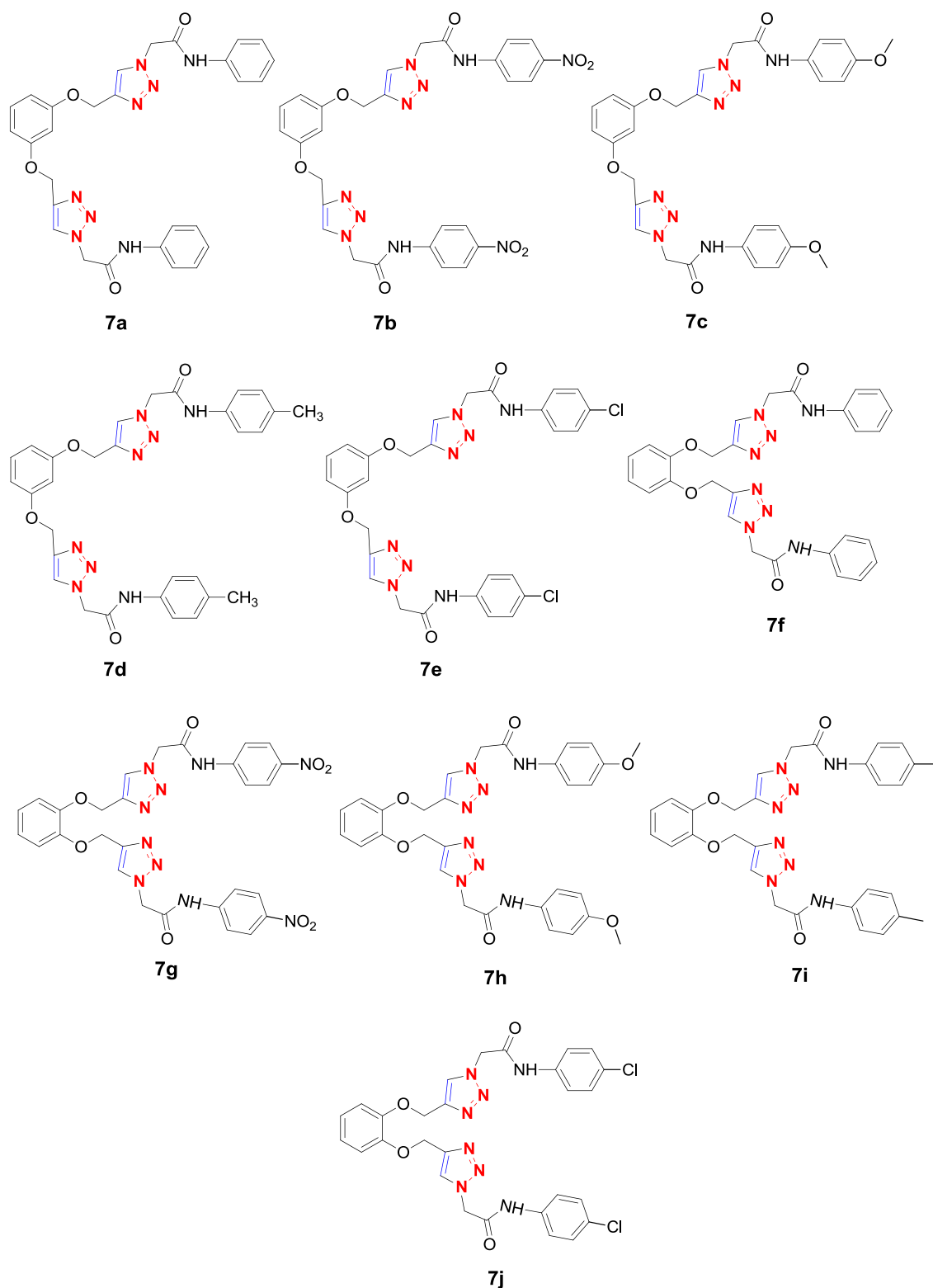


Fig. 3. Structures of newly synthesized aryloxy bridged and amide linked dimeric 1,2,3-triazoles (7a-j).

phosphorylation with ~100% inhibition against MCF-7 cell line. The results of inhibition of EGFR tyrosine kinase phosphorylation by newly synthesized compounds were summarized in Table 2.

From Table 2, the compound 7h was displayed most potent activity among all the synthesized compounds with 88.34% inhibition of EGFR tyrosine kinase phosphorylation. The compounds 7d and 7j also acts as good inhibitors of EGFR-TK Phosphorylation with 76.87% and 72.68%

inhibition, respectively against MCF-7. The immunoblot analysis of the EGFR against MCF-7 cancer cell line for potent compounds were shown in Fig. 4.

Fig. 4 reveals that, the inhibition of EGFR tyrosine kinase phosphorylation after exposure to compounds 7j (Lane 1), 7d (Lane 2), 7h (Lane 3) and Gefitinib (Lane 4) for 48 h. From all these results, we can conclude that, the compound 7h was found as a good inhibitor of EGFR-

**Table 1**  
*In vitro* antiproliferative activity of the synthesized derivatives (7a–j).

Entry	IC <sub>50</sub> Value (μM)		
	MCF-7	A549	MCF-10A
7a	NA	7.05 ± 3.93	NT
7b	NA	2.22 ± 0.07	NT
7c	NA	2.34 ± 0.74	NT
7d	6.01 ± 3.09	NA	NT
7e	6.13 ± 3.81	NA	NT
7f	NA	NA	NT
7g	NA	NA	NT
7h	4.18 ± 3.18	NA	33.44
7i	6.70 ± 4.13	5.56 ± 2.05	NT
7j	2.80 ± 2.47	5.61 ± 3.35	14.00
Gefitinib	2.97 ± 1.09	2.11 ± 0.88	NT

NA: Not Applicable; NT: Not Tested.

**Table 2**

The percentage EGFR-TK inhibitory activity of the active anti-proliferative agents against MCF-7 cell line.

Compound	% EGFR-TK Inhibition of MCF-7 <sup>a</sup>
7d	76.87 ± 0.68
7e	32.62 ± 0.10
7h	88.34 ± 0.09
7i	28.22 ± 0.42
7j	72.68 ± 0.18
<sup>b</sup> Gefitinib	~100*

\* Absence of immunoblot in Lane 4 of MCF-7 showed complete inhibition of EGFR phosphorylation.

<sup>a</sup> The data were means from at least three independent experiments at a single dose of 10 μM concentration.

<sup>b</sup> Gefitinib was used as a standard antiproliferative drug at 10 μM concentration.

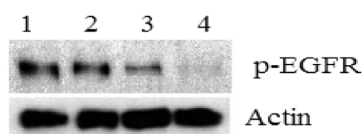


**Fig. 4.** Immunoblot analysis of the EGFR in MCF-7 cancer cell line.

TK Phosphorylation as it displays 88% inhibition of EGFR-TK Phosphorylation against MCF-7 cancer cell line, which is found to be close to the standard drug Gefitinib. Therefore, the compound 7h acts as a potent antiproliferative agent due to its ability to inhibit EGFR tyrosine kinase phosphorylation.

Furthermore, in support to biological activities, the molecular docking was also performed in Maestro 9.1 using the Induced Fit Docking (IFD) protocol (Schrodinger LLC)<sup>18</sup> for newly synthesized compounds against EGFR kinase domain (PDB entry: 3W33). The IFD combines the Glide docking program for ligand flexibility and the Prime program for receptor flexibility. In the refinement module of Prime for protein, the side chain degrees of freedom are mainly sampled, while minor backbone movements are allowed through minimization. The docking results indicated that the compounds were held in the active pocket by combination of various hydrogen and hydrophobic interactions with EGFR enzyme. The compounds 7d, 7h and 7j showed binding affinity and pose similar to that of standard drug Gefitinib (Figs. 5a and 5b).

It was found from literature that all EGFR inhibitors make a weak interaction with amino acids residue Met793. Thus the constraints were defined during IFD studies that all compounds must form the H-bond with Met793 and it is surprising that ether linkage of most of the compounds shows the H-bond with Met793. This interaction also confirms our compound design strategy for ether linkage, which act as

hydrogen bond acceptor (Fig. 6). These compounds also showed H-bonding with amino acid residues Phe723, Lys745, Arg841, Thr854, and Asp855 which support ligand-enzyme complex. It is also visualized that one of the triazole ring and phenyl ring strengthen the stability of complex by making  $\pi$ -cation interaction with amino acid residue Lys745 and/or Arg841.

A drug can be said as successful if it having good efficacy as well as an acceptable ADME profile. ADME properties prediction is one of the important as well as widely known pharmacokinetic parameter for the prediction of the oral bioavailability of any drug. A compound is also considered to be an orally active drug as well as obeys the Lipinski's rule of five if there is only one violation is observed out of the following four criteria's:  $\text{miLog } P$  (octanol–water partition coefficient)  $\leq 5$ , molecular weight  $\leq 500$ , number of hydrogen bond acceptors  $\leq 10$  and number of hydrogen bond donors  $\leq 5$ . Therefore, to know the oral bioavailability, Lipinski violations and drug likeness properties of all the newly synthesized aryloxy bridged and amide linked substituted dimeric 1,2,3-triazolyl compounds (7a–j), herein, we have predicted and studied the *in silico* ADME properties, % of absorption and drug-likeness model score. The results of *in silico* ADME prediction studies including Lipinski violations, % of absorption and drug-likeness model score were summarized in Table S2 (Supporting Information). According to obtained results, most of the predictions were found to be within the acceptable range. All the synthesized compounds exhibited moderate to good % ABS ranging from 29.74 to 61.36%. Drug likeness score was also calculated in order to achieve biological activity of compound. Most of the compounds from the synthesized series shows positive drug likeness score. All the results show that the compounds possess average to good potential for the development as orally active drug molecule.

In conclusion, the aryloxy bridged and amide linked substituted dimeric 1,2,3-triazole hybrids (7a–j) were synthesized and evaluated for antiproliferative activity against two human cancer cell lines (MCF-7 and A549). Eight compounds of the series were displayed good to excellent antiproliferative activities against tested human cancer cell lines. The compounds, 7d, 7e, 7h, 7i and 7j were observed as potent antiproliferative agents against human breast cancer cell line (MCF-7), whereas, the compounds, 7a, 7b, 7c, 7i and 7j have been revealed promising antiproliferative activity against human lung cancer cell line (A-549). Furthermore, the study of EGFR tyrosine kinase phosphorylation inhibition also carried out with active antiproliferative agents against MCF-7 cell line. The results of this study show that the compounds, 7d, 7h and 7j were acts as active EGFR tyrosine kinase phosphorylation inhibitors. In support to this study, the newly synthesized compounds have been also shows good results of molecular docking as well as ADME properties were observed in acceptable range. From the above observations it can be conclude that newly synthesized aryloxy bridged and amide linked substituted dimeric 1,2,3-triazole hybrids (7a–j) offers an attractive lead series for the discovery of novel antiproliferative agents as well as EGFR tyrosine kinase phosphorylation inhibitors.

## Declaration of Competing Interest

The authors declare that they have no known competing financial interests or personal relationships that could have appeared to influence the work reported in this paper.

## Acknowledgments

Authors are also thankful to the Head, Department of Chemistry, Dr. Babasaheb Ambedkar Marathwada University, Aurangabad-431 004, India for providing laboratory facility.

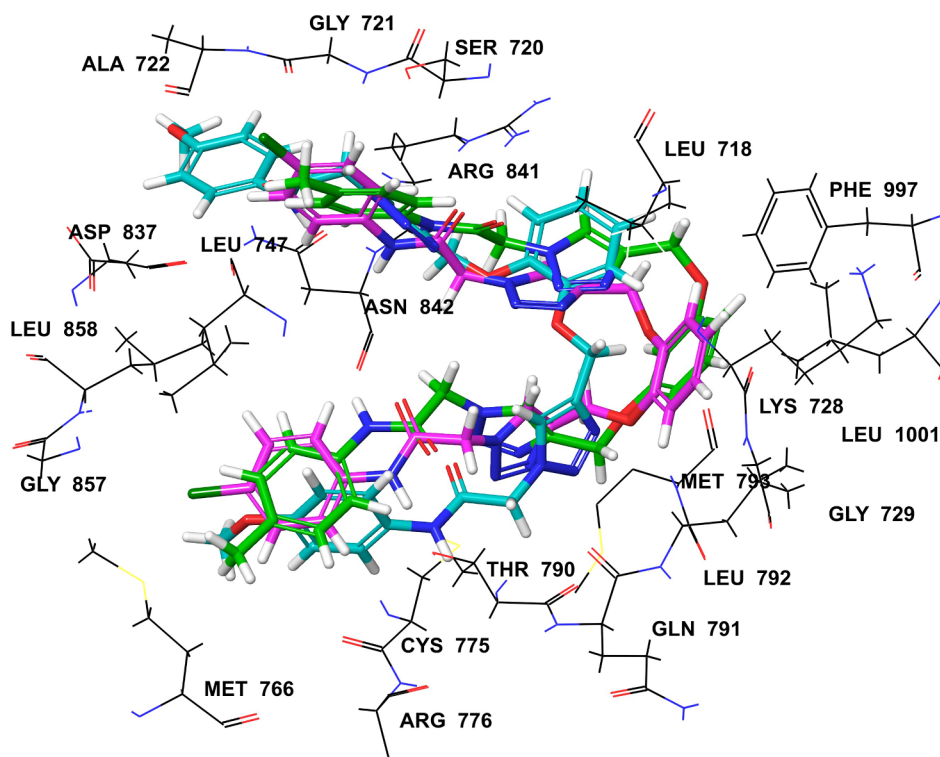


Fig. 5a. The superimposition of docking pose of compound 7d (green coloured), 7h (light blue coloured) and 7j (magenta coloured) into the active site of EGFR enzyme.

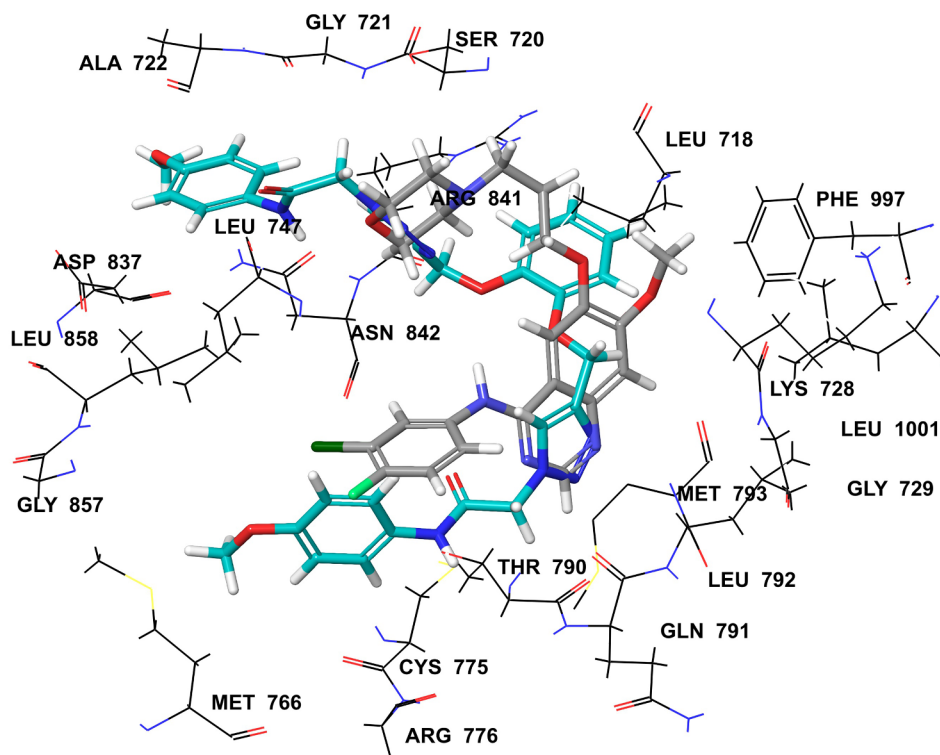
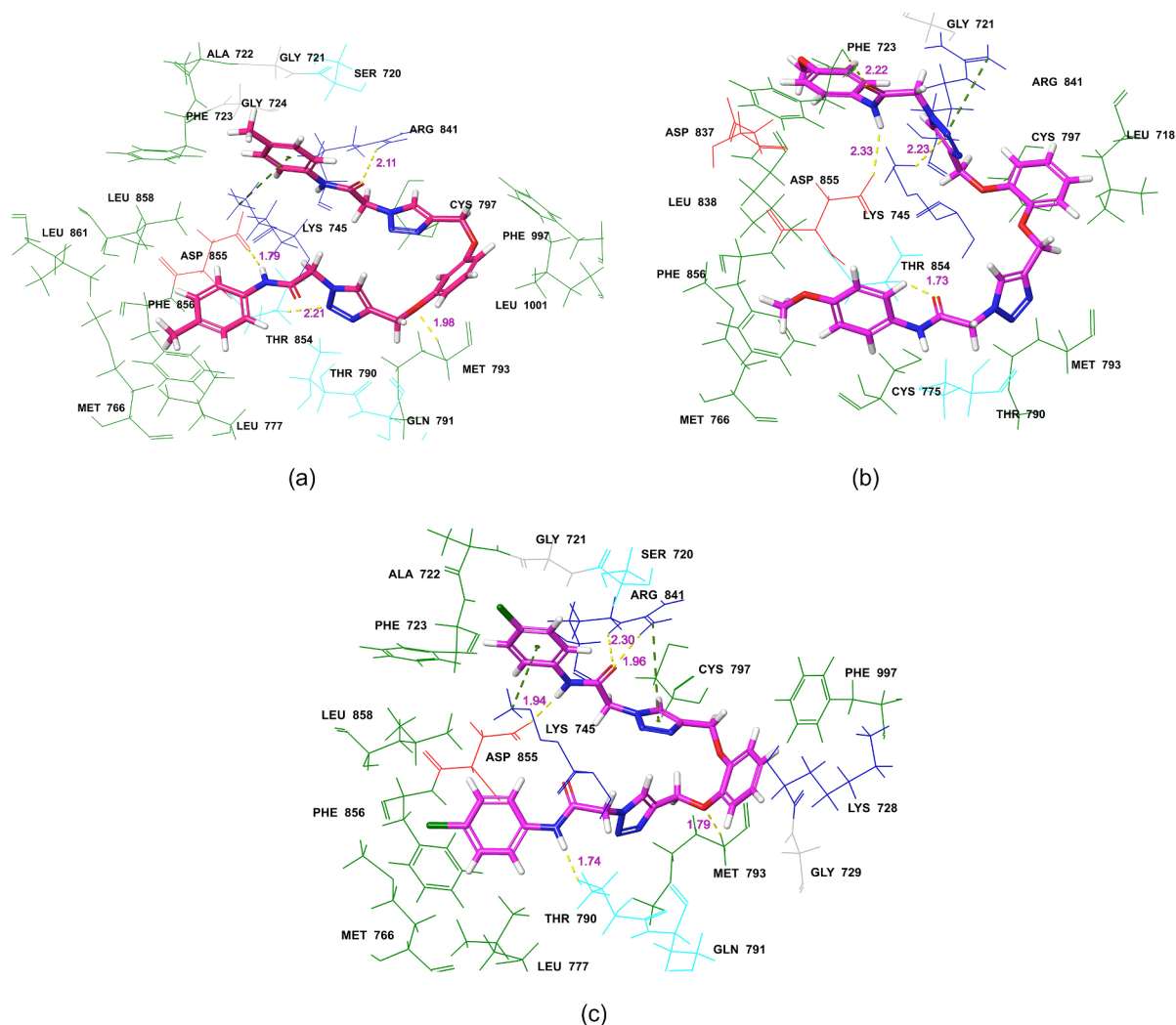


Fig. 5b. The superimposition of docking pose of standard Gefitinib (gray coloured) and compound 7h (light blue coloured) into the active site of EGFR enzyme.



**Fig. 6.** The docking pose of compounds (a) **7d**, (b) **7h** and (c) **7j** into the active site of EGFR enzyme. The yellow coloured dotted line indicate H-bond and green coloured dotted line indicate  $\pi$ -cation interaction. The magenta coloured numerical indicates the distance of H-bonds. The amino acids are coloured according to their property like hydrophobicity, charged and polar (Gray colour: Cysteine, green colour: hydrophobic, cyan colour: polar uncharged, blue colour: positives, and red colour: negatives).

## Appendix A. Supplementary data

Supplementary data to this article can be found online at <https://doi.org/10.1016/j.bmcl.2019.08.022>.

## References

- Kaur M, Singh P. Targeting tyrosine kinase: development of acridone-pyrrole-oxindole hybrids against human breast cancer. *Bioorg Med Chem Lett*. 2019;29:32–35.
- Bari SB, Adhikari S, Surana SJ. Tyrosine kinase receptor inhibitors: a new target for antiproliferative drug development. *J PharmaSciTech*. 2012;1:36–45.
- Yagublu V, Ahmadova Z, Hajiyeva Y, Hafner M, Keese M. Combination of the EGFR tyrosine kinase inhibitor AG1478 and 5-FU: no synergistic effect on EGFR phosphorylation, cell proliferation and apoptosis induction. *Antiproliferative Res*. 2013;33:3753–3758.
- Hadden MK, Blagg BSJ. Dimeric approaches to anti-cancer chemotherapeutics. *Antiproliferative Agents Med Chem*. 2008;8:807–816.
- (a) Ahmad K, Khan MKA, Baig MH, Imran M, Gupta GK. Role of azoles in cancer prevention and treatment: present and future perspectives. *Anti-Cancer Agents Med Chem*. 2018;18:46–56  
(b) Jabir NR, Firoz CK, Bhushan A, Tabrez S, Kamal MA. The use of azoles containing natural products in cancer prevention and treatment: an overview. *Anti-Cancer Agents Med Chem*. 2018;18:6–14  
(c) Bhardwaj A. A review on azole derivatives as potent anticancer agents. *Int J Chemtech Res*. 2018;11:154–175.
- (a) Lal K, Yadav P. Recent advancements in 1,4-disubstituted-1H-1,2,3-triazoles as potential antiproliferative agents. *Antiproliferative Agents Med Chem*. 2018;18:21–23  
(b) Kumar S, Kumar SV, Gupta GK, et al. Antibacterial, tyrosinase and DNA photocleavage studies of some triazolynucleosides. *Nucleos Nucleot Nucl*. 2017;36:543–551  
(c) Huang RZ, Liang GB, Li MS, et al. Synthesis and discovery of asiatic acid based 1,2,3-triazole derivatives as antitumor agents blocking NF- $\kappa$ B activation and cell migration. *Med Chem Commun*. 2019;10:584–597  
(d) Bebenek E, Tomanek MK, Chrobak E, Latocha M, Boryczka S. Novel triazoles of 3-acetylbutelin and betulone as anticancer agents. *Med Chem Res*. 2018;27:2051–2061.
- (a) Kolb HC, Sharpless KB. The growing impact of click chemistry on drug discovery. *Drug Discov Today*. 2003;8:1128–1137  
(b) Tornøe CW, Christensen C, Meldal M. Peptidotriazoles on solid phase: [1,2,3]-triazoles by regioselective copper(I)-catalyzed 1,3-dipolar cycloadditions of terminal alkynes to azides. *J Org Chem*. 2002;67:3057–3064  
(c) Rostovtsev VV, Green LG, Fokin VV, Sharpless KB. A stepwise Huisgen cycloaddition process: copper(I)-catalyzed regioselective ligation of azides and terminal alkynes. *Angew Chem Int Ed*. 2002;41:2596–2599  
(d) Kolb HC, Finn MG, Sharpless KB. Click chemistry: diverse chemical function from a few good reactions. *Angew Chem Int Ed*. 2001;40:2004–2021.
- Dheer D, Singh V, Shankar R. Medicinal attributes of 1,2,3-triazoles: current developments. *Bioorg Chem*. 2017;71:30–54.
- Prachayasittikul V, Pingaew R, Anuwongcharoen N, et al. Discovery of novel 1,2,3-triazole derivatives as antiproliferative agents using QSAR and *in silico* structural modification. *SpringerPlus*. 2015;4:571–592.
- Ashwini N, Garg M, Mohan CD, et al. Synthesis of 1,2-benzisoxazole tethered 1,2,3-triazoles that exhibit antiproliferative activity in acute myeloid leukemia cell lines by inhibiting histone deacetylases, and inducing p21 and tubulin acetylation. *Bioorg Med Chem*. 2015;23:6157–6165.
- Pokhodylo N, Shyyka O, Matychuk V. Synthesis of 1,2,3-triazole derivatives and

- evaluation of their antiproliferative activity. *Sci Pharm.* 2013;81:663–676.
- Stefely JA, Palchadhuri R, Miller PA, et al. *N*-((1-Benzyl-1*H*-1,2,3-triazol-4-yl)methyl) arylamide as a new scaffold that provides rapid access to antimicrotubule agents: synthesis and evaluation of antiproliferative activity against select cancer cell lines. *J Med Chem.* 2010;53:3389–3395.
  - Tiew KC, Dou D, Teramoto T, et al. Inhibition of Dengue virus and West Nile virus proteases by click chemistry-derived benz[*d*]isothiazol-3(2*H*)-one derivatives. *Bioorg Med Chem.* 2012;20:1213–1221.
  - (a) Anand A, Naik RJ, Revankar HM, Kulkarni MV, Dixit SR, Joshi SD. A click chemistry approach for the synthesis of mono and bis aryloxy linked coumarinyl triazoles as anti-tubercular agents. *Eur J Med Chem.* 2015;105:194–207  
(b) Kant R, Kumar D, Agarwal D, et al. Synthesis of newer 1,2,3-triazole linked chalcone and flavone hybrid compounds and evaluation of their antimicrobial and cytotoxic activities. *Eur J Med Chem.* 2016;113:34–49.
  - Compound 7a:** White solid; Yield: 92%; Mp: 228–230 °C; IR ( $\nu_{\max}$  cm<sup>-1</sup>) 3268 (N–H, amide), 1677 (C=O, amide); <sup>1</sup>H NMR (400 MHz, DMSO-*d*<sub>6</sub>,  $\delta_{\text{H}}$  ppm) 5.17 (s, 4H, O-CH<sub>2</sub>), 5.36 (s, 4H, N-CH<sub>2</sub>), 6.68 (dd, 2H, Ar-H), 6.77 (s, 1H, Ar-H), 7.08 (t, 2H, Ar-H), 7.20 (t, 1H, Ar-H), 7.32 (d, 4H, Ar-H), 7.57 (d, 4H, Ar-H), 8.27 (s, 2H, triazolyl-H), 10.48 (s, 2H, amido-H); <sup>13</sup>C NMR (100 MHz, CDCl<sub>3</sub>,  $\delta_{\text{C}}$  ppm) 57.5, 66.3, 106.8, 112.6, 124.5, 129.1, 131.6, 134.2, 135.3, 143.7, 147.7, 164.6, 169.4; HRMS (ESI) calcd. For C<sub>28</sub>H<sub>27</sub>N<sub>8</sub>O<sub>4</sub> [M+H]<sup>+</sup>: 539.2155; found: 539.2160. **Compound 7b:** Dark creamish solid; Yield: 94%; Mp: 128–130 °C; IR ( $\nu_{\max}$  cm<sup>-1</sup>) 3254 (N–H, amide), 1679 (C=O, amide); <sup>1</sup>H NMR (500 MHz, DMSO-*d*<sub>6</sub>,  $\delta_{\text{H}}$  ppm) 5.19 (s, 4H, O-CH<sub>2</sub>), 5.46 (s, 4H, N-CH<sub>2</sub>), 6.68 (dd, 2H, Ar-H), 6.78 (s, 1H, Ar-H), 7.23 (t, 1H, Ar-H), 7.84 (d, 4H, Ar-H), 8.26 (d, 4H, Ar-H), 8.29 (s, 2H, triazolyl-H), 11.09 (s, 2H, amido-H); <sup>13</sup>C NMR (100 MHz, DMSO-*d*<sub>6</sub>,  $\delta_{\text{C}}$  ppm) 52.8, 61.6, 102.1, 107.9, 119.6, 125.6, 126.9, 130.6, 143.1, 143.2, 145.0, 159.8, 165.9; LCMS (ESI) calcd. For C<sub>28</sub>H<sub>25</sub>N<sub>10</sub>O<sub>8</sub> [M+H]<sup>+</sup>: 629.1857; found: 629.1. **Compound 7c:** Dark yellowish solid; Yield: 91%; Mp: 197–198 °C; IR ( $\nu_{\max}$  cm<sup>-1</sup>) 3267 (N–H, amide), 1667 (C=O, amide); <sup>1</sup>H NMR (400 MHz, DMSO-*d*<sub>6</sub>,  $\delta_{\text{H}}$  ppm) 3.91 (s, 6H, OCH<sub>3</sub>), 5.34 (s, 4H, O-CH<sub>2</sub>), 5.50 (s, 4H, N-CH<sub>2</sub>), 6.85 (dd, 2H, Ar-H), 6.95 (s, 1H, Ar-H), 7.09 (d, 4H, Ar-H), 7.40 (t, 1H, Ar-H), 7.68 (d, 4H, Ar-H), 8.44 (s, 2H, triazolyl-H), 10.53 (s, 2H, amido-H); <sup>13</sup>C NMR (100 MHz, DMSO-*d*<sub>6</sub>,  $\delta_{\text{C}}$  ppm) 52.6, 55.6, 61.5, 102.0, 107.8, 114.5, 121.3, 126.7, 130.5, 131.9, 142.9, 156.0, 159.8, 164.1; HRMS (ESI) calcd. For C<sub>30</sub>H<sub>31</sub>N<sub>8</sub>O<sub>6</sub> [M+H]<sup>+</sup>: 599.2367; found: 599.2363. **Compound 7d:** Pale yellow solid; Yield: 93%; Mp: 206–208 °C; IR ( $\nu_{\max}$  cm<sup>-1</sup>) 3267 (N–H, amide), 1661 (C=O, amide); <sup>1</sup>H NMR (400 MHz, DMSO-*d*<sub>6</sub>,  $\delta_{\text{H}}$  ppm) 2.26 (s, 6H, CH<sub>3</sub>), 5.17 (s, 4H, O-CH<sub>2</sub>), 5.33 (s, 4H, N-CH<sub>2</sub>), 6.67 (dd, 2H, Ar-H), 6.77 (s, 1H, Ar-H), 7.14 (d, 4H, Ar-H), 7.22 (t, 1H, Ar-H), 7.47 (s, 4H, Ar-H), 8.26 (s, 2H, triazolyl-H), 10.39 (s, 2H, amido-H); <sup>13</sup>C NMR (100 MHz, DMSO-*d*<sub>6</sub>,  $\delta_{\text{C}}$  ppm) 20.9, 52.7, 61.5, 102.0, 107.8, 119.7, 126.8, 129.8, 130.5, 133.3, 136.4, 143.0, 159.8, 164.4; HRMS (ESI) calcd. For C<sub>30</sub>H<sub>31</sub>N<sub>8</sub>O<sub>4</sub> [M+H]<sup>+</sup>: 567.2468; found: 567.2469. **Compound 7e:** Light yellowish solid; Yield: 89%; Mp: 250–253 °C; IR ( $\nu_{\max}$  cm<sup>-1</sup>) 3275 (N–H, amide), 1685 (C=O, amide); <sup>1</sup>H NMR (400 MHz, DMSO-*d*<sub>6</sub>,  $\delta_{\text{H}}$  ppm) 5.20 (s, 4H, O-CH<sub>2</sub>), 5.40 (s, 4H, N-CH<sub>2</sub>), 6.70 (dd, 2H, Ar-H), 6.80 (s, 1H, Ar-H), 7.25 (t, 1H, Ar-H), 7.43 (d, 4H, Ar-H), 7.65 (d, 4H, Ar-H), 8.30 (s, 2H, triazolyl-H), 10.66 (s, 2H, amido-H); <sup>13</sup>C NMR (125 MHz, DMSO-*d*<sub>6</sub>,  $\delta_{\text{C}}$  ppm) 52.7, 61.5, 102.0, 107.8, 121.3, 126.8, 127.8, 129.3, 134.6, 137.8, 142.9, 159.8, 164.9; HRMS (ESI) calcd. For C<sub>28</sub>H<sub>25</sub>Cl<sub>2</sub>N<sub>8</sub>O<sub>4</sub> [M+H]<sup>+</sup>: 607.1376; found: 607.1372. **Compound 7f:** Creamish white solid; Yield: 90%; Mp: 190–192 °C; IR ( $\nu_{\max}$  cm<sup>-1</sup>) 3267 (N–H, amide), 1669 (C=O, amide); <sup>1</sup>H NMR (400 MHz, DMSO-*d*<sub>6</sub>,  $\delta_{\text{H}}$  ppm) 5.20 (s, 4H, O-CH<sub>2</sub>), 5.37 (s, 4H, N-CH<sub>2</sub>), 6.96 (dd, 2H, Ar-H), 7.11 (t, 2H, Ar-H), 7.23 (dd, 2H, Ar-H), 7.36 (t, 4H, Ar-H), 7.60 (d, 4H, Ar-H), 8.27 (s, 2H, triazolyl-H), 10.50 (s, 2H, amido-H); <sup>13</sup>C NMR (100 MHz, DMSO-*d*<sub>6</sub>,  $\delta_{\text{C}}$  ppm) 52.7, 62.1, 114.8, 119.7, 121.8, 124.3, 126.9, 129.4, 138.9, 143.1, 148.4, 164.7; HRMS (ESI) calcd. For C<sub>28</sub>H<sub>27</sub>N<sub>8</sub>O<sub>4</sub> [M+H]<sup>+</sup>: 539.2155; found: 539.2143. **Compound 7g:** Blackish green solid; Yield: 92%; Mp: > 270 °C; IR ( $\nu_{\max}$  cm<sup>-1</sup>) 3244 (N–H, amide), 1673 (C=O, amide); <sup>1</sup>H NMR (400 MHz, DMSO-*d*<sub>6</sub>,  $\delta_{\text{H}}$  ppm) 5.20 (s, 4H, O-CH<sub>2</sub>), 5.45 (s, 4H, N-CH<sub>2</sub>), 6.96 (d, 2H, Ar-H), 7.21 (d, 2H, Ar-H), 7.82 (d, 4H, Ar-H), 7.97 (d, 4H, Ar-H), 8.25 (s, 2H, triazolyl-H), 11.09 (s, 2H, amido-H); <sup>13</sup>C NMR (100 MHz, DMSO-*d*<sub>6</sub>,  $\delta_{\text{C}}$  ppm) 62.4, 70.4, 116.7, 119.8, 122.1, 125.7, 131.0, 143.2, 145.1, 148.6, 151.6, 163.0; HRMS (ESI) calcd. For C<sub>28</sub>H<sub>25</sub>N<sub>10</sub>O<sub>8</sub> [M+H]<sup>+</sup>: 629.1857; found: 629.1850. **Compound 7h:** Creamish white solid; Yield: 89%; Mp: 213–215 °C; IR ( $\nu_{\max}$  cm<sup>-1</sup>) 3267 (N–H, amide), 1670 (C=O, amide); <sup>1</sup>H NMR (400 MHz, DMSO-*d*<sub>6</sub>,  $\delta_{\text{H}}$  ppm) 3.71 (s, 6H, OCH<sub>3</sub>), 5.16 (s, 4H, O-CH<sub>2</sub>), 5.29 (s, 4H, N-CH<sub>2</sub>), 6.89 (d, 4H, Ar-H), 6.92 (dd, 2H, Ar-H), 7.19 (dd, 2H, Ar-H), 7.48 (d, 4H, Ar-H), 8.22 (s, 2H, triazolyl-H), 10.33 (s, 2H, amido-H); <sup>13</sup>C NMR (100 MHz, DMSO-*d*<sub>6</sub>,  $\delta_{\text{C}}$  ppm) 52.6, 55.8, 62.1, 114.4, 114.6, 121.2, 121.4, 127.0, 132.0, 143.1, 148.4, 156.1, 164.2; HRMS (ESI) calcd. For C<sub>30</sub>H<sub>31</sub>N<sub>8</sub>O<sub>6</sub> [M+H]<sup>+</sup>: 599.2367; found: 599.2366. **Compound 7i:** Light yellow solid; Yield: 91%; Mp: 232–235 °C; IR ( $\nu_{\max}$  cm<sup>-1</sup>) 3265 (N–H, amide), 1660 (C=O, amide); <sup>1</sup>H NMR (400 MHz, DMSO-*d*<sub>6</sub>,  $\delta_{\text{H}}$  ppm) 2.26 (s, 6H, CH<sub>3</sub>), 5.17 (s, 4H, O-CH<sub>2</sub>), 5.32 (s, 4H, N-CH<sub>2</sub>), 6.94 (d, 2H, Ar-H), 7.14 (d, 4H, Ar-H), 7.21 (d, 2H, Ar-H), 7.46 (d, 4H, Ar-H), 8.23 (s, 2H, triazolyl-H), 10.39 (s, 2H, amido-H); <sup>13</sup>C NMR (125 MHz, DMSO-*d*<sub>6</sub>,  $\delta_{\text{C}}$  ppm) 20.9, 52.6, 62.1, 114.8, 119.7, 121.8, 126.8, 129.7, 133.2, 136.4, 143.1, 148.4, 164.4; HRMS (ESI) calcd. For C<sub>30</sub>H<sub>31</sub>N<sub>8</sub>O<sub>4</sub> [M+H]<sup>+</sup>: 567.2468; found: 567.2471. **Compound 7j:** Yellowish solid; Yield: 85%; Mp: 253–255 °C; IR ( $\nu_{\max}$  cm<sup>-1</sup>) 3255 (N–H, amide), 1680 (C=O, amide); <sup>1</sup>H NMR (400 MHz, DMSO-*d*<sub>6</sub>,  $\delta_{\text{H}}$  ppm) 5.17 (s, 4H, O-CH<sub>2</sub>), 5.37 (s, 4H, N-CH<sub>2</sub>), 6.66 (dd, 2H, Ar-H), 7.23 (dd, 2H, Ar-H), 7.39 (d, 4H, Ar-H), 7.62 (d, 4H, Ar-H), 8.27 (s, 2H, triazolyl-H), 10.63 (s, 2H, amido-N-H); <sup>13</sup>C NMR (100 MHz, DMSO-*d*<sub>6</sub>,  $\delta_{\text{C}}$  ppm) 52.7, 61.6, 121.3, 121.4, 127.0, 127.9, 129.3, 129.5, 130.7, 137.9, 143.0, 164.9; HRMS (ESI) calcd. For C<sub>28</sub>H<sub>25</sub>Cl<sub>2</sub>N<sub>8</sub>O<sub>4</sub> [M+H]<sup>+</sup>: 607.1376; found: 607.1377.
  - Dofe VS, Sarkate AP, Azad R, Gill CH. Novel quinoline-based oxadiazole derivatives induce G2/M arrest and apoptosis in human breast cancer MCF-7 cell line. *Res Chem Intermed.* 2017;43:7331–7345.
  - Johnson AC, Murphy BA, Matelis CM, et al. Activator protein-1 mediates induced but not basal epidermal growth factor receptor gene expression. *Mol Med.* 2000;6:17–27.
  - Scherman W, Day T, Jacobson MP, Friesner RA, Farid R. Novel procedure for modelling ligand/receptor induced fit effects. *J Med Chem.* 2006;49:534–553.